Mechanics of Advanced Composite Structures

Journal homepage: https://macs.semnan.ac.ir/

Semnan University

ISSN: 2423-7043

Research Article

Microstructure & Mechanical Properties Evaluation of Al6082 /AlSi10Mg Composite for Light Weight Structural Applications

Burlakanti Subramanyam *, Pitchaipillai Periyasamy

Department of Mechanical Engineering, St. Peter's Institute of Higher Education & Research, Avadi, Chennai, 600054, India.

ARTICLE INFO

Article history:

Received: 2023-08-09
Revised: 2023-12-10
Accepted: 2024-01-12

Keywords:

Stir casting technique;

Microstructure analysis;

Mechanical properties;

SEM analysis;

EDS analysis;

XRD analysis.

ABSTRACT

The main objective of this research work is to provide lightweight and high-strength materials for structural engineering applications. In general, the mechanical properties of pure Al6082 components are less as compared to the AlSi10Mg components. This work aims to study and improve the mechanical properties of the Al6082/AlSi10Mg composite. The composite, produced by the stir casting technique, stands out for its mechanical performance and microstructure. The findings shed light on the composite's suitability for different uses in sectors like aerospace, automotive, and marine. The outcomes of microstructure and mechanical properties can give significant evidence about whether a composite is appropriate for a given application. This data can be used to make well-informed choices about the composite's suitability for particular applications and to direct future advancements in its mechanical strength. The experimental work was carried out with the composition of Al6082 raw material and AlSi10Mg fresh powder. The weight percentage (Wt. %) of AlSi10Mg is considered with 0.5 % for sample S1, 1.0 % for sample S2, and 0.0 % for sample S3. The microstructure analyses performed that, the S1 sample showed fine microstructure with major porosity, the S2 sample showed coarse structure with minor porosity and the S3 sample showed fine microstructure with minor porosity. The microstructural investigation shows that the silica particles were evenly distributed throughout the aluminum matrix, which ensured that the composites' ultimate tensile strength, hardness, and impact strength had been increased. The mechanical properties of samples are evaluated with tensile, compression, impact, and hardness tests. The tensile strength of the S2 sample (127 MPa) is high as compared to the S1 sample (110 MPa) due to less porosity, fine grain microstructure, and high Ti element presence in the S2 sample. The compressive strength of the S2 sample (143.3 MPa) is high as compared to the S1 sample (117.1 MPa) due to the fine grain microstructure and high Ti element in the S2 sample. The impact strength of the S2 sample (4.4 J) is high compared to the S1 sample (4.0 J). The microhardness tested at 0.5 Kgf load, 63.7 HV for the S1 sample, 65.1 HV for the S2 sample, and 46.3 HV for the S the 3 sample. Further, the microhardness test was conducted at 1.0 Kgf load., the values are 54.7 HV for the S1 sample, 59.7 HV for the S2 sample, and 38.3 HV for the S3 sample. From the findings, it is stated that the S2 sample performed an excellent mechanical property as compared to the S1 and S3 samples due to more wt. % of Ti and Al in the S2 sample. SEM examination revealed that the S1 sample has more pits and cracks as compared to the S2 and S3 samples. SEM, EDS, and XRD analyses were performed and displayed outstanding results. XRD analysis revealed the same elemental presence of EDS analysis. The research work is carried out in a systematic procedure and a comparison is made of the test results with the available existing results by the researchers. Compared to other compositions of available existing research work this Al6082 / AlSi10Mg is also suggestable for the development of lightweight structural applications.

*** Corresponding author.**
E-mail address: *bsm52052@gmail.com*

Cite this article as:

Subramanyam, B. and Periyasamy, P., 2024. Microstructure & Mechanical Properties Evaluation of Al6082 /AlSi10Mg Composite for Light Weight Structural Applications. *Mechanics of Advanced Composite Structures*, 11(2), pp. 309-320

https://doi.org/10.22075/MACS.2024.31464.1547

1. Introduction

Al6082 is a common aluminum alloy used in the manufacture of structural components with high strength, due to its excellent corrosion resistance, formability, and weldability. Manganese, magnesium, silicon, and iron are the primary alloying components of Al6082. The aerospace, automotive, and building industries frequently use Al6082.

An alloy made of aluminum, silicon, and magnesium called AlSi10Mg is used to make casting components and 3D printing. Aluminum gains stronger, harder, and more thermally stable mechanical properties as a result of the addition of silicon and magnesium. Due to its excellent castability and corrosion resistance, AlSi10Mg is frequently used in the automotive, aerospace, and electrical industries. AlSi10Mg has a high silicon content, which enhances fluidity during casting and produces castings with better surface finish and dimensional accuracy. AlSi10Mg typically contains 10% silicon, 0.4% magnesium, 0.6% iron, 0.4% copper, 0.1% copper, 0.15% manganese, and the balance is aluminum. The alloy is renowned for having a high thermal conductivity, which qualifies it for uses requiring effective heat dissipation. AlSi10Mg is the perfect material for lightweight structural components like brackets, housings, and engine parts due to its high strength and low weight. Because of its excellent corrosion resistance, it can be used in harsh environments like the sea. Alloys made of aluminum are strong, castable, and highly ductile [1].

Surface hardness value, compressive strength, microstructure, and tensile strength of stir-casted alloys are tested with one another in order to establish the ideal stirrer speed [2]. The specimen's geometry affects its mechanical properties, and heat treatment greatly improves the composite's malleability and energy dissipation while greatly lowering its compressive yield strength [3]. The maximum hardness value for an alloy matrix specimen without reinforcements was 56.8 HRB and the results proved that slight reduction in hardness by adding the SiC wt. % [4]. AA6082 developed equiaxed grains and smaller grains as a result of SiC particulates [5]. The aluminum and aluminum alloys exhibit specific strength and properties at high temperatures [6]. Desired material properties in accordance with their applications are achieved by using magnesium alloys [7]. AZ31 magnesium alloy matrix composites with Graphene Oxide (GO) reinforcement outperformed their unreinforced counterparts in terms of strength, toughness, and plasticity [8]. In comparison to unground granite samples, the addition of finely ground granite exhibits greater compressive strength [9].

The mechanical properties of MMNCs are significantly influenced by the distribution of GNPs in metal matrices and the bonding between GNPs and metal matrices [10]. Excellent thermal insulating and strength qualities are achieved by the composites made from waste granite scrap [11]. The tests' outcome showed that the engineering qualities of granitic rocks vary widely [12]. High Na_2O and Al content necessitate a sintering step in order to recover these values [13]. By using the stir casting technique at different stirrer speeds and duration time, an Al-SiC MMC material by adding 10% SiC was produced. The outcomes of the hardness test revealed a relationship between stirring time, speed, and the composite's hardness. The uniform hardness values were reached after 10 minutes of stirring at 600 rpm, but after that, the properties started to deteriorate once more. By increasing the stirring time and speed, SiC was dispersed more evenly throughout the Al matrix. It was discovered that SiC distributions were more uniform at 600 rpm and 10 minutes of stirring [14]. When using materials like steel, iron, silicon carbide, and composites without chills, the grain size enlarges over time, but when using copper chills, fine grain structure, uniform dispersoid distribution, and strong matrix-dispersoid bonding are the results [15]. To align the microstructure, a microstructural analysis of the modified A356 was performed. Microstructure is made up of eutectic silicon particles with rounded, less angular shapes distributed in a matrix of aluminum solid solution, as well as Mg_2Si particles [17]. For 12% cerium oxide, the compressive strength increased from 83 MPa to 176 MPa, and the microhardness also increased up to 40% [18]. The composite prepared with AA6061 as the matrix material and a novel combination of Silicon Carbide (SiC), Fly ash, and Graphite (Gr) as reinforcing materials, revealed a fine-grain structure [19]. Microstructure analysis reveals that the 25mm diameter casting has better matrix and reinforcement bonding than the 50 and 75mm castings. According to the investigation's findings, stir casting can successfully reinforce fly ash and B4C in an Al-4.5 wt.% Cu alloy to produce hybrid MMCs [20]. It was found that reinforced boron carbide composite had a maximum tensile strength and hardness of 10%. By increasing boron carbide in the matrix material; toughness, ductility, and density are all reduced. The aluminum alloy AA2014 can be successfully developed by stir casting and boron carbide as reinforcement. The microstructure results showed that B4C was distributed correctly in the AA2014 matrix material [21].

The UTS of the composite rises as Fly Aah (FA) content increases. A discernible increase in

strength is seen. The sample with a 6-weight percentage FA content was given its maximum strength. The strength began to decrease once the FA content reached 6 weight percent. This is because the matrix's high concentration of FA content might not have been distributed evenly [22]. A Hybrid Metal Matrix (HMM) composite is made up of SiC, Coconut Shell Ash (CSA), and FA particles in various sizes, and has improved tensile strength significantly. It has been noted that samples A and D each have CSA concentrations of 0%, 5%, and 10% at 173 MPa, 194 MPa, and 213 MPa, respectively. As the percentage of CSA particles in the matrix rises, the matrix alloy significantly gains strength [23]. Depending on the composition's weight ratio, 3 compositions are used for casting, including 90% Al + 2.5% Basalt fiber ash + 7.5% Fly ash, 90% Al + 5% Basalt fiber ash + 5% Fly ash, and 90% Al + 7.5% Basalt fiber ash + 2.5% Fly ash. According to the experimental findings, the first composition has a higher tensile strength than the other two compositions. [24]. The observed improvement in corrosion resistance of SiC particulate-reinforced nanocomposites is due to the good bond integrity of SiC particles with AA7178 [31]. The weight percentage of nano TiO_2 had an overall impact on the coefficient of friction and wear rate of 60.95% and 57.33%, respectively [32].

Fly ash that has been received can be used to reinforce subsequent materials. It has a low density and good mechanical characteristics. A356 alloy and fly ash composite's compressive strength has increased in a satisfactory manner [25]. The specimen with 0.2% zinc oxide reinforcement proved the greatest mechanical properties [26]. The granite specimens' Uniaxial Compressive Strength (UCS) slightly rises for samples heated to 200°C, but it then linearly falls for samples heated to temperatures between 200°C and 800°C. Up to 800°C, the heat treatment temperature causes a reduction in Young's modulus before remaining constant [27]. Utilizing all of these experimental findings with 178 different granites, it was determined how the granites behave mechanically in compression and tension. The measured parameters varied significantly, with the exception of bulk density. About 15% more than the average value of all the granites in the database, which is 138 MPa, this rock has a compressive strength of about 158 MPa [28]. The reinforced zinc oxide (0.2%) sample proved the highest tensile strength (23.9 kg/mm^2), hardest surface (134.4 HV), flattest grain distribution, and most brittle fracture [29]. Samples of composites have reinforcement weight fractions of 3% fly ash, which is constant, and varying weights of 5, 10, and 15% Al_2O_3 [30].

The reinforcement of TiB_2 particulates (0 to 9 %) with AA7075 has a UTS value of 275-300 MPa [34]. The reinforcement of 1.5% Al_2O_3p with A356 resulted in a UTS of 265 MPa [36]. The reinforced MgOp (1.5-5 wt.%) with A356 performed 850-1000 MPa of UTS [39]. The reinforced RHAp (3-12 wt.%) with AlSi10Mg performed the value of 170-175 MPa UTS [40].

A study of Electron Backscatter Diffraction (EBSD) demonstrated the evolution of coarser grains into finer grains. The textures of all the samples appeared to be utterly arbitrary. Neither the SiC addition nor the processing conditions appear to have a significant impact on the texture [43]. The first time quantifying the size and distribution of Mg_2Si particles in the Al matrix was made possible using the small-angle diffraction technique [44]. Al, SiC, and CuO peaks are validated by the XRD pattern [45].

The majority of the researchers have made great efforts to introduce novel materials. The approach of different researchers has been different as they have taken different materials and their compositions and also different manufacturing methods/processes.

This research work is aimed to introduce the varying weight percentage (wt.%) of AlSi10Mg fresh powder in Al6082 raw material by using a stir casting process and the mechanical properties are evaluated on a composite sample.

2. Materials and Methods

The research is carried out using a methodology that includes building a sample with the preferred composition of Al6082 / AlSi10Mg by using a stir-casting process. After the casting, the material undergoes machining as per the required dimensions of test samples.

2.1. Elemental Composition of Al6082 Raw Material & AlSi10Mg Fresh Powder

The following Tables 1 and 2 represent the elemental composition of Al6082 raw material and AlSi10Mg fresh powder.

Table 1. Elemental composition of Al6082 raw material

Element	Si	Al	Fe	Ca	Mg	Na	K	O	Total
Weight %	0.5	95	0.2	0.0	0.3	0.1	0.0	3.7	100

Table 2. Elemental composition of AlSi10Mg fresh powder

Element	Si	Al	Fe	Ti	Mg	N_2	Zn	O	Total
Weight %	9	90	0.2	0.1	0.2	0.2	0.1	0.2	100

2.2. Manufacturing of Al6082 / AlSi10Mg Test Samples

Stir casting is used to prepare Al6082 / AlSi10Mg samples which are reinforced with 0.5% and 1.0% wt.% under vacuum conditions. Figures 1-6 represent the steps followed to prepare the test samples.

- Adding Al6082 material in the crucible.
- Pre-heating the furnace and placing the crucible.
- Adding AlSi10Mg powder into the crucible.
- Stirring the composite.
- Die Preparation of Al6082 / AlSi10Mg composite.

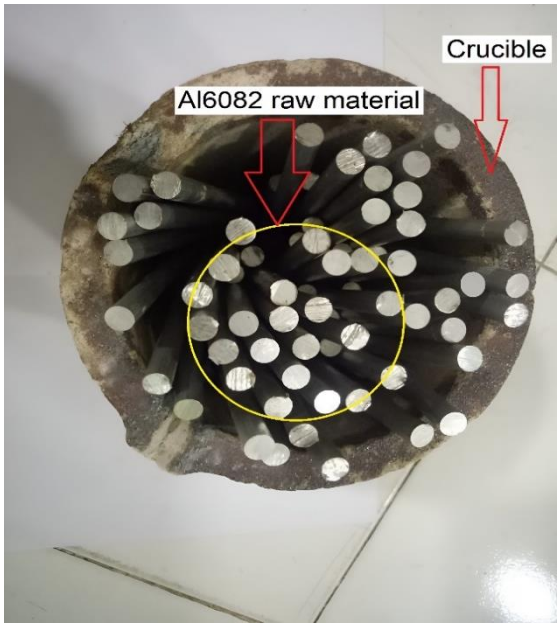

Fig. 1. Al6082 raw material preparation for stir casting

Figure 1 represents the raw material (Al6082) placed in a crucible for stir casting.

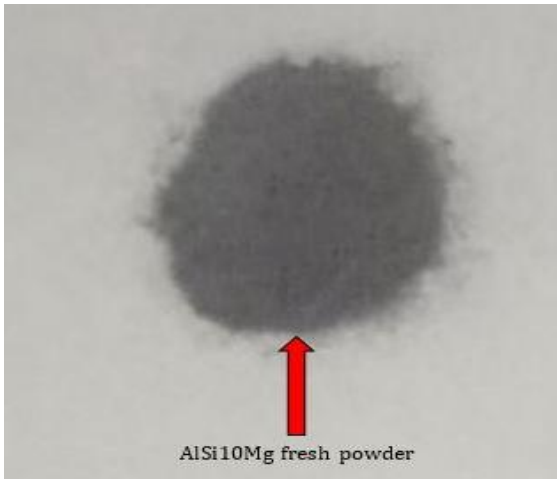

Fig. 2. AlSi10Mg fresh powder for reinforcement

Figure 2 shows the AlSi10Mg fresh powder to use as a reinforcement with different wt.%

2.3. Stir Casting Specifications

The make and origin of the experimental setup is Ultra furnace-1000, Made in Korea and assembled in India. The specifications followed to conduct the experiment with 850^{0}C furnace temperature maintained, Capacity used for 500g, Stirring maintained with a normal speed of 600 RPM, stirring time: 5 minutes, pouring time: 2 minutes, and pre-heating of die: 300^{0}C. Stir casting technique used to prepare the composition of materials. Samples were prepared by using Al6082 and AlSi10Mg powder with varying weight percentages (wt.%). The sample S1 was prepared with 99.5 wt.% of Al6082 and 0.5 wt.% of AlSi10Mg. Sample S2 prepared with 99.0 wt.% of Al6082 and 1.0 wt.% of AlSi10Mg. Sample S3 prepared with 100.0 wt.% of Al6082 and 0.0 wt.% of AlSi10Mg.

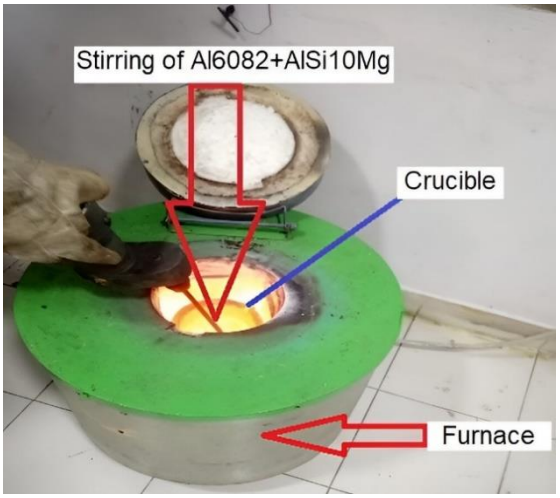

Fig. 3. Stir casting setup (Stirring of Al6082 / AlSi10Mg in stir casting setup)

Figure 3 indicates the stirring of Al6082 raw material and AlSi10Mg fresh powder for the preparation of test samples. Figure 4 shows the sequential steps to prepare the test samples.

Fig. 4. Stir casting setup and pouring of Al6082 / AlSi10Mg molten metal into a die

The sequential process from raw material to preparation of composite has been carried out with four steps. Step 1, indicates the placing of Al6082 raw material in the furnace along with the crucible. Step 2, shows that adding AlSi10Mg to melted Al6082 raw material. Step 3 shows the stirring of Al6082+AlSi10Mg material and Step 4 indicates pouring molten material into die.

The following Table 3 represents the wt.% of Al6082 raw material and wt.% of AlSi10Mg fresh powder.

Table 3. Sample number with respect to composition

Composition → / Sample No. ↓	Al6082 wt. %	AlSi10Mg wt. %
S1	99.5	0.5
S2	99.0	1.0
S3	100.0	0.0

Figure 5 shows the unmachined Al6082 / AlSi10Mg samples with respect to samples S1 and S2.

Fig. 5. Stir cast Al6082 / AlSi10Mg unmachined material

The S1 & S2 stir-casted material has undergone machining and turning for the preparation of test samples as per the requirement.

Fig. 6. Test samples of stir-casted Al6082 / AlSi10Mg composition

Figure 6 shows the machined samples prepared for the required tests.

3. Results and Discussion

To begin with, the microstructure analysis is carried out after the machining of samples. The experimental results were performed with microstructure analysis, tensile test, compression test, impact test, and hardness test.

3.1. Microstructure Analysis

The microstructure analysis has been carried out by taking AlSi10Mg fresh powder, Al6082 raw sample (S3), and the stir-casted S1 & S2 samples. Figure 7 shows the SEM image of AlSi10Mg fresh powder. The S1 sample shows a coarse grain boundary structure in Fig. 8, whereas the S2 and S3 samples show a fine grain boundary structure in Figs. 9 and 10. The porosity is minimal in the S2 and S3 samples as compared to the S1 sample.

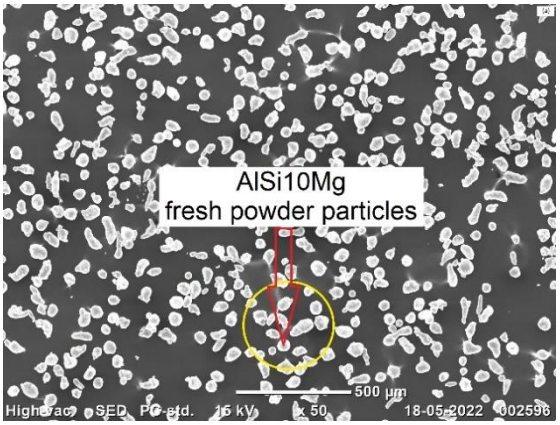

Fig. 7. SEM image of AlSi10Mg fresh powder

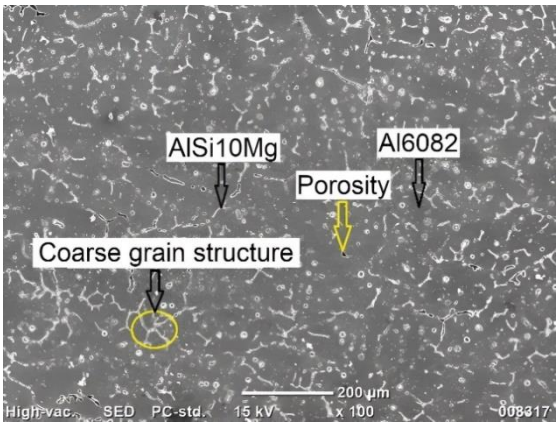

Fig. 8. SEM image of S1 sample

There is no substantial amount of clustering and agglomeration of reinforcement observed in the microstructure examination. The experimental results of the S1, S2, and S3 samples also performed a coarse grain structure and fine grain structure with major porosity in the S1 sample and minor porosity in the S2 sample identified in the SEM analysis. The scanning electron microscope (SEM) analysis showed that

the reinforcement particles were evenly dispersed across the surface of the aluminum matrix [41]. There is less discernible clustering or agglomeration of reinforcement. The clusters of grains in the S1 sample are less as compared to the S2 sample.

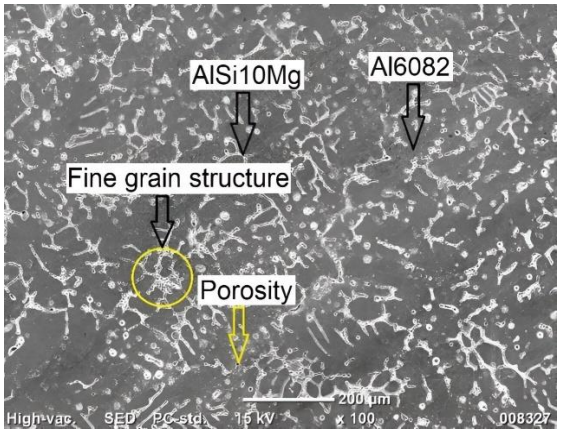

Fig. 9. SEM image of S2 sample

It is clear from the micrographs that the microstructure is primarily made up of roughly equiaxed α-Mg dendritic structures [16]. The experimental setup used for SEM is Model (6000 Plus), Make (JEOL). As seen in Figs. 8 and 9, the white color lines indicate the reinforced AlSi10Mg material and the other shows Al6082 raw material. Figure 10 shows the fine-grain structure with less porosity. SEM analysis revealed that the basic alloy had more pitting and cracking than the reinforced composite [31].

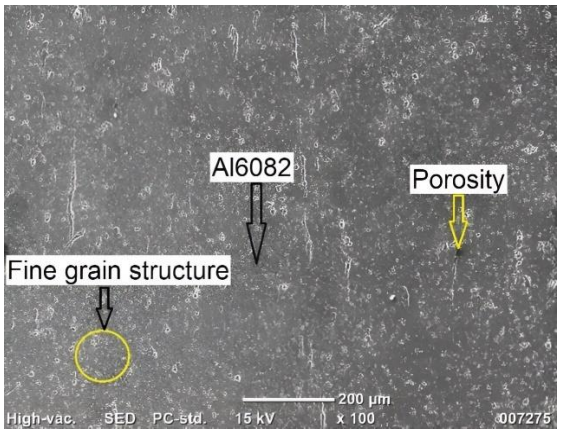

Fig. 10. SEM image of S3 sample

The SEM image in microstructure examination shows a fine grain structure with the nano TiO_2 particles with concentrations of 1%, 2%, and 3%, which were reinforced with an AA7178 metal matrix composite using a stir casting method [42]. According to the microstructural analyses, the addition of nanoparticles reduces grain size [43].

3.2. Tensile Test

Standards of ASTM 577M have been used for the tensile test by UTM. Least count of displacement: 0.1 mm, crosshead speed: 1.0 mm/minute, software: Auto instruments, FIE. The make and origin of the experimental setup is FIE, Maharashtra, Kolhapur, Made in India. The following Fig. 11 indicates the tensile test specimen parameters in "mm". The tensile test is used to precisely measure properties such as ultimate tensile strength.

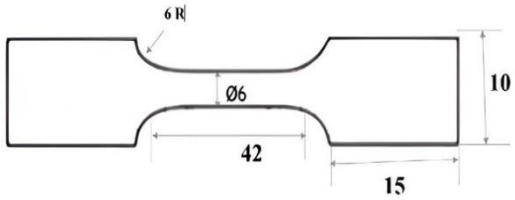

Fig. 11. Parameters of Tensile test specimen

The tensile test is conducted under the specified circumstances. The tensile test results are shown in Table 4.

Table 4. Tensile test results

Sample No.	Ultimate Tensile Strength (MPa)			
	Sample 1	Sample 2	Sample 3	Average Value
S1	120	122	90	110.7
S2	110	150	120	127.0

The tensile test was performed with S1 & S2 at each 3 samples. The S2 sample proved a greater strength as compared to the S1 sample. The UTS of the S2 sample (127 MPa) is increased as compared to the S1 sample (110 MPa) due to fine grain structure and Ti element presence in the S2 sample. As compared to the reinforcement of Grinder stone (10 to 20 %) with Al6063 having a UTS of 165 MPa [35].

3.3. Compression Test

A compression test was conducted by UTM with the standards of ASTM 577M. Least count of displacement: 0.1 mm, crosshead speed: 1.0 mm/minute, software: Auto instruments, FIE. The make and origin of the experimental setup is FIE, Maharashtra, Kolhapur, Made in India.

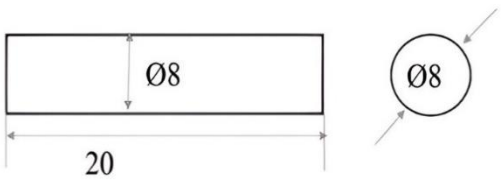

Fig. 12. Parameters of Compression test specimen

The compression test is carried out as per the given parameters. Figure 12 provides the specimen parameters for the compression test. The following table 5 displays the experimental outcomes.

Table 5. Compression test results

Sample No.	Test samples	Ult. / Break load (KN)	Max. Displacement (mm)	Ult. Stress (MPa)
S1	S1-1	6.33	4.9	124.7
	S1-2	6.73	5.9	132.6
	S1-3	4.78	4.3	94.2
S2	S2-1	7.32	5.8	144.1
	S2-2	6.96	5.8	137.1
	S2-3	7.55	4.4	148.7

The experimental results of the compression test revealed that the S2 samples performed maximum ultimate stress (avg. of 143.3 MPa) as compared to the S1 sample (avg. of 117.1 MPa).

3.4. Impact Test

The S1 and S2 samples' composition was tested for impact. The specimen parameters for the impact test are shown in Fig. 13. The make and origin of the experimental setup is Krystal equipment, Made in India, Kolhapur, Maharashtra.

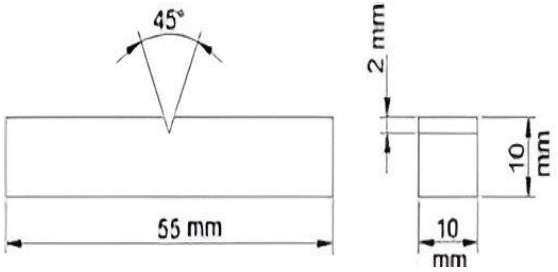

Fig. 13. Parameters of Impact test specimen

For the test, each composition produced 3 samples. The results of the impact test are displayed in Table 6.

Table 6. Impact test results

Sample No.	Impact strength (J)			
	Sample 1	Sample 2	Sample 3	Average Value
S1	3.8	4.7	3.5	4.0
S2	5.4	4.0	3.9	4.4

The experimental results showed that the S1 samples had minimum impact strength as compared to the S2 samples.

3.5. Microhardness Test

ASTM E384 is the standard used for the microhardness Test. The experimental work has been carried out with the applied load of 0.5 Kgf and 1 Kgf with a dwell time of 10 Sec. The test is conducted on each sample S1, S2, and S3. The make and origin of the experimental setup is Wilson Wolpert, made in Germany, Model MVD-401. The following Fig. 14 shows the microhardness test results.

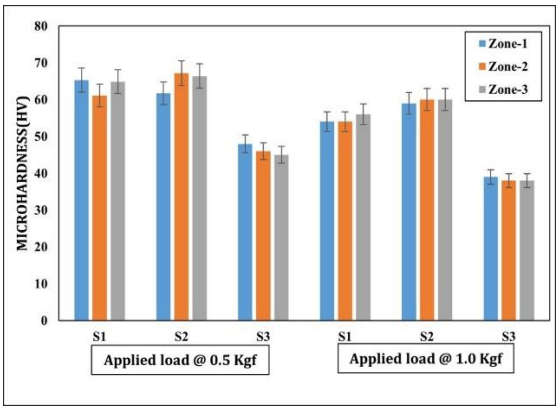

Fig. 14. Microhardness test for S1, S2 & S3 sample

The hardness value is observed to increase as the weight percentage of the composition S2 sample increases. Furthermore, S3 is seen to have a lower hardness value than S1 and S2, which have higher hardness values.

The hardness and tensile strength of the metal matrix composite are enhanced by increasing the volume fraction of the reinforcing materials [33]. The reinforcement of TiB_2 particulates (0 to 9 wt.%) with AA7075 has a hardness value of 120-130 VHN [34]. The reinforcement of Grinder stone (10 to 20 wt.%) with Al6063 has a hardness value of 75 BHN 35]. The reinforcement of 1.5 wt.% Al_2O_3p with A356 showed a hardness value of 120-135 BHN [36]. The reinforced B_4Cp (3-10 wt.%) with Al2024 performed 93.07 BHN hardness value [37]. The hardness value of 71 HVN was achieved for the reinforcement of 10 wt.% of Granite with LM6 material [38]. The reinforced MgOp (1.5-5 wt.%) with A356 performed 65-75 BHN hardness value [39]. The reinforced RHAp (3-12 wt.%) with AlSi10Mg performed 80-90 BHN hardness value [40].

4. SEM Analysis

The experimental setup used for SEM is Model (6000 Plus), Make (JEOL). The SEM analysis has been conducted on the microhardness tested samples of 1.0 Kgf for the S1 and S2 as shown in Figs. 15 and 16. It is observed that the S2 sample produces good strength without any defects as compared to the S1 sample.

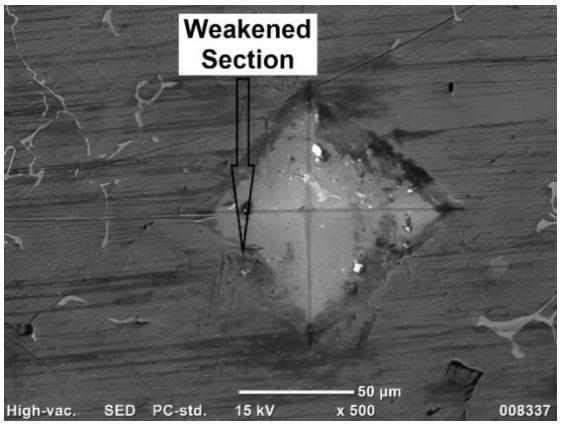

Fig. 15. SEM image of Microhardness tested S1 sample

Figure 15 shows the weakened section in the microhardness test conducted S1 sample in an SEM analysis.

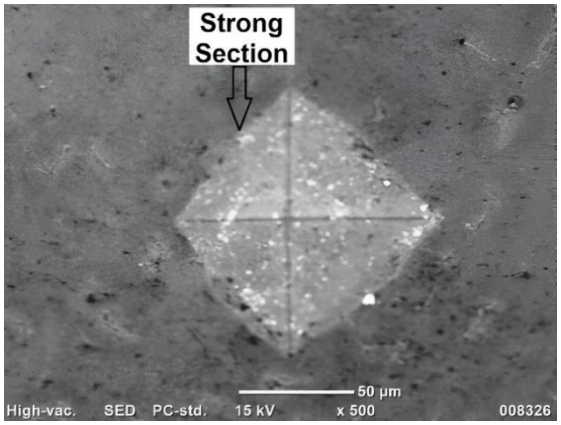

Fig. 16. SEM image of Microhardness tested S2 sample

Figure 16 shows the strong section in the microhardness test conducted S2 sample in an SEM analysis. From the SEM analysis, the S2 sample has greater hardness as compared to the S1 sample due to the elemental presence of Ti and the fine grain structure of the S2 sample.

5. EDS Analysis

Model (6000 Plus), Make (JEOL), is the experimental setup used for EDS.

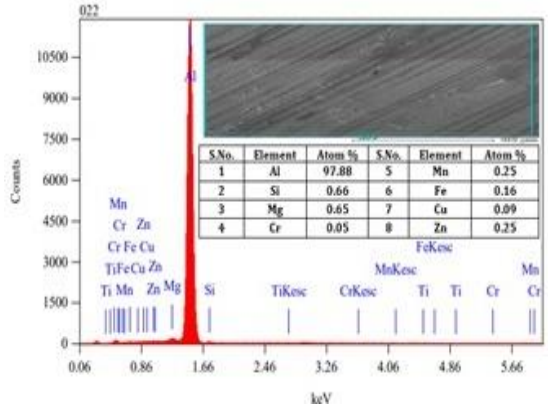

Fig. 17. EDS plot for test sample S1

The following conditions were used for the EDS analysis. Live Time: 10.00 sec, Dead Time: 9%, Counting Rate: 12057 cps, Energy Range: 0 - 20 keV. The EDS plot of Figs. 17 and 18 display the mass percentage of both samples in a respectable manner.

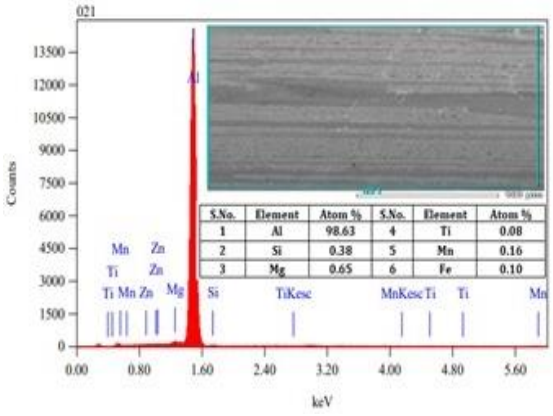

Fig. 18. EDS plot for test sample S2

The S1 and S2 samples were subjected to the EDS analysis. Comparing the S2 sample to the S1 sample, it can be seen that the S2 sample produced excellent results. The analysis using SEM showed that the reinforcement particles were evenly dispersed over the aluminum matrix surface. A product with a finer grain structure was produced by adding nanoparticles to composites, according to studies using electron backscatter diffraction (EBSD). The material developed with the reinforcement of SiC and TiO_2 nanoparticles in AA7178 material by using a stir casting process [41]. The results of the SEM and EDS analysis guarantee that the chromium and silicon carbide particles are present and distributed throughout the matrix grain structure, with little to no cluster formation [46]. The finding of EDS confirms that SiC and Mo particles are present in the Al alloy [47].

6. XRD Analysis

Model (XRD-7000), Make (SHIMADZU), is the experimental setup used for XRD analysis.

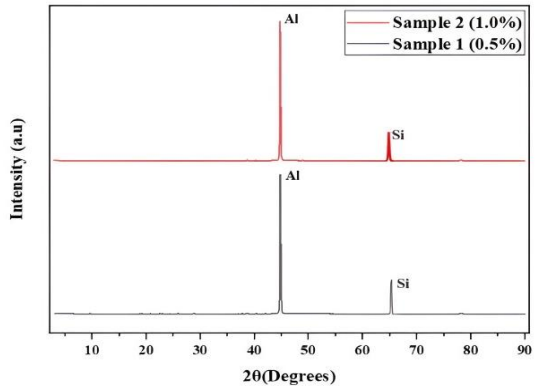

Fig. 19. XRD of S1 & S2 sample

The XRD analysis has been carried out for S1 and S2 samples. Figure 19 shows the presence of Al & Si elements in both the S1 and S2 samples. These elements are also confirmed by the EDS analysis [48-50]. It is observed that the S2 sample proved greater diffraction data as compared to S1. The S1 sample shows weaker peak intensities than the S2 sample. The intensity (a. u) value is taken from 0 to 4000 on the Y-axis and 2θ (Degrees) on the X-axis.

7. Conclusions

This study has successfully investigated the development of mechanical properties characterization of Al6082/AlSi10Mg stir-casted specimen using the stir casting technique. The results show that the mechanical properties of the composite material are greatly improved by the addition of AlSi10Mg particles. According to the microstructure analysis, the AlSi10Mg particles were evenly dispersed throughout the Al6082 matrix, which contributed to the composite material's enhanced mechanical properties.

- Due to more wt.% of Ti in the S2 sample, the microstructure of the S2 sample formed is a fine grain structure with minor porosity as compared to the S1 sample.
- The Si content of the S1 sample (0.68 wt.%) is high as compared to the S2 sample (0.39 %) but the mechanical properties of the S2 sample are high as compared to the S1 sample due to less porosity, fine grain structure, and presence of more Ti in S2 sample.
- The tensile strength of the S2 sample performed at 127 MPa as compared to the S1 sample performed at 110 MPa.
- The compressive strength of the S2 sample performed with 143 MPa whereas the S1 sample performed with 117 MPa. It is observed that the compressive strength is higher than the tensile strength for the S1 & S2 samples.
- While increasing the wt.% of AlSi10Mg fresh powder, the impact strength of the S2 sample increased.
- The harness value of the S2 sample is high as compared to the S1 and S3 samples at different locations and different load conditions due to its elemental composition and grain structure.
- In tensile, compression, impact, and microhardness tests, the composite material outperformed the pure Al6082 matrix in terms of hardness and mechanical strength.

The results of this study show that the stir casting technique has the potential to be used to create high-performance Al6082/AlSi10Mg composite materials with enhanced mechanical properties. When high strength is needed, such materials can be used in the automotive, aerospace, and marine industries.

Funding Statement

This research did not receive any specific grant from funding agencies in the public, commercial, or not-for-profit sectors.

Conflicts of Interest

The author declares that there is no conflict of interest regarding the publication of this article.

References

[1] Kumar, D., Singh, S. and Angra, S., 2023. Dry sliding wear and microstructural behavior of stir-cast Al6061-based composite reinforced with cerium oxide and graphene nanoplatelets. *Wear*, *516*, p.204615. doi.10.1016/j.wear.2022.204615.

[2] Arunkumar, S., Ramakrishna, C.S., Alphin, M.S., Muraliraja, R., Kumar, T.V., Vishwakarma, B., Agrawal, V. and Yadav, A.S., 2023. Optimization of stirrer speed on mechanical properties of aluminium graphite stir cast. *Materials Today: Proceedings*. doi.10.1016/j.matpr.2023.03.379.

[3] Prakash, K. and Singh, N.K., 2023. Behaviour of a stir casted aluminium hybrid composite under compressive and bending loads. *Materials Today: Proceedings*. doi.10.1016/j.matpr.2023.05.18.

[4] Mishra, D. and Nanda, A.K., 2023. Experimental investigation on mechanical properties of stir casted aluminum SiC metal matrix composites. *Materials Today: Proceedings,* 74, pp.1023-1027. doi.10.1016/j.matpr.2022.11.412.

[5] Surendarnath, S., Ramesh, G., Ramachandran. T., Dharmalingam, R. and Murugapoopathi, S., 2022. Dry sliding wear behavior of aluminum alloy 6082-Sic composites through ex-situ casting process. Proceedings of the Institute of Mechanical Engineers, Part J: Journal of Engineering Tribology, 237 (8). pp.1-10. doi.10.1177/13506501221142651.

[6] Pise, D., Shravankumar, C. and TVVLN., R., 2020. An overview on aluminum metal matrix composite for automobile

application. Proceedings of Mechanical Engineering Research Day 2020, pp.14-15.

[7] Prasad, S.S., Prasad, S.B., Verma, K., Mishra, R.K., Kumar, V. and Singh, S., 2022. The role and significance of Magnesium in modern day research-A review. *Journal of Magnesium and Alloys*, *10*(1), pp.1-61. doi.10.1016/j.jma.2021.05.012.

[8] Tahaghoghi, M., Zarei-Hanzaki, A., Jalali, M.S. and Abedi, H.R., 2022. Improved strength and plasticity of magnesium matrix nanocomposites reinforced by carbonaceous nanoplatelets and micro-clusters. *Journal of Materials Research and Technology, 21,* pp. 2797-2814. doi.10.1016/j.jmrt.2022.10.083.

[9] Stempkowska, A., Gawenda, T., Chajec, A. and Sadowski, Ł., 2022. Effect of Granite Powder Grain Size and Grinding Time of the Properties of Cementitious Composites. *Materials*, *15*(24), p.8837. doi.10.3390/ma15248837.

[10] Tabandeh-Khorshid, M., Kumar, A., Omrani, E., Kim, C. and Rohatgi, P., 2020. Synthesis, characterization, and properties of graphene reinforced metal-matrix nanocomposites. *Composites Part B: Engineering*, *183*, pp.1-7.

[11] Paul, S.C., Miah, M.Y., Gafur, A. and Das, R.C., 2017. Study of thermal properties of granite powder (scrap) reinforced polyester resin composite. *Journal of Advanced J Chemical Engineering, 6(3),* pp.1-5. doi.10.4172/2090-4568.1000159.

[12] Yadav, R.K. and Anurag, A., 2014. A Study on Variation in Mineralogical and Strength Characteristics of Some Granitic Rocks. *International Journal of Engineering Research & Technology, 3(1),* pp.505-511.

[13] Samal, S., Ray, A.K. and Bandopadhyay, A., 2013. Proposal for resources, utilization and processes of red mud in India—A review. *International Journal of Mineral Processing*, *118,* pp.43-55. doi.10.1016/j.minpro.2012.11.001.

[14] Balasivanandha Prabu, S., Karunamoorthy, L., Kathiresan, S. and Mohan, B., 2006. Influence of stirring speed and stirring time on distribution of particles in cast metal matrix composite. *Journal of Materials Processing Technology, 171(2),* pp. 268-273. doi.10.1016/j.jmatprotec.2005.06.071.

[15] Anantha Prasad, M.G. and Bandekar, N., 2015. Study of Microstructure and Mechanical Behavior of Aluminum / Garnet/Carbon Hybrid Metal Matrix Composites (HMMCs) Fabricated by Chill Casting Method. *Journal of Materials Science and Chemical Engineering, 3,* pp.1-8. doi.10.4236/msce.2015.33001.

[16] Anand, N., Ramachandran, K.K. and Bijulal, D., 2021. Microstructural, mechanical and tribological characterization of vacuum stir cast Mg-4Zn/Si3N4 magnesium matrix nanocomposite. *Materials Today: Proceedings,* 46, pp.9387-9391. doi.10.1016/j.matpr.2020.03.053.

[17] Dhanasekaran, R. and Kumar, K.S., 2015. Microstructure, mechanical properties of A356/Li aluminum alloy fabrication by stir casting method. *International Journal of Applied Engineering Research, 10(50),* pp. 416-419.

[18] Anand Babu, V., Kumaravel, A. and Manikandan, R., 2023. Microstructure, mechanical and wear characteristics of CeO2-Mg metal matrix composites. *Proceedings of the Institution of Mechanical Engineers, Part E: Journal of Process Mechanical Engineering, 237(2),* pp.430-440. doi.10.1177/09544089221139592.

[19] Chechi, P., Maurya, S.K., Prasad, R. and Manna, A., 2022. Microstructural and mechanical characterization of stir cast Al-SiC/Flyash/Graphite hybrid metal matrix composite. *Materials Today: Proceedings*, *64*, pp.637-642. doi.10.1016/j.matpr.2022.05.150.

[20] Lokesh, G.N., Prashanth, K.P., Prasad, G.P. and Venkatesha, B.K., 2022. Mechanical and microstructure evaluation of stir cast Al-4.5% Cu alloy reinforced fly ash/boron carbide hybrid metal matrix composites. *Materials Today: Proceedings*, *54*, pp.486-491. doi.10.1016/j.matpr.2021.11.131.

[21] Dwivedi, S.P., 2020. Microstructure and mechanical behaviour of Al/B4C metal matrix composite. *Materials Today: Proceedings*, *25*, pp.751-754. doi.10.1016/j.matpr.2019.08.244.

[22] Ravichandran, M., Balasubramanian, M., Chairman, C.A., Marichamy, S., Dhinakaran, V. and Stalin, B., 2020 December. Mechanical properties of Fly ash reinforced Aluminium matrix composites. *In IOP Conference Series: Materials Science and Engineering* (Vol. 988, No. 1, p. 012095). *IOP Publishing.* doi.10.1088/1757-899X/988/1/012095.

[23] Devanathan, R., Ravikumar, J., Boopathi, S., Selvam, D.C. and Anicia, S.A., 2020. Influence in Mechanical Properties of Stir Cast Aluminium (AA6061) Hybrid Metal matrix Composite (HMMC) with Silicon Carbide, Fly

Ash and Coconut coir Ash Reinforcement. *Materials Today: Proceedings, 22(4),* pp.3136-3144. doi.10.1016/j.matpr.2020.03.450.

[24] Kumaravel, S., and Mohanraj, D., 2019. Production and Mechanical Properties of Fly ash and Basalt ash reinforced Al 6061 composites. *Indian Journal of Engineering, 16,* pp.276-283.

[25] Kulkarni, S.G., Meghnani, J.V. and Lal, A., 2014. Effect of Fly Ash Hybrid Reinforcement on Mechanical Property and Density of Aluminium 356 Alloy. *Procedia Materials Science, 5,* pp. 746-754. doi.10.1016/j.mspro.2014.07.324.

[26] Puspitasari, P., Soepriyanto, O.R., Sasongko, M.I.N. and Dika, J.W., 2018. Mechanical and physical properties of aluminium-silicon (Al-Si) casting alloys reinforced by Zinc Oxide (ZnO). *In MATEC Web of Conferences (Vol. 204, p. 05003). EDP Sciences*. doi.10.1051/matecconf/201820405003.

[27] Chen, Y.L., Wang, S.R., Ni, J., Azzam, R. and Fernandez-Steeger, T.M., 2017. An experimental study of the mechanical properties of granite after high temperature exposure based on mineral characteristics. *Engineering Geology, 220,* pp.234-242. doi.10.1016/j.enggeo.2017.02.010.

[28] Domede, N., Parent, T. and Sellier, A., 2019. Mechanical behaviour of granite: a compilation, analysis and correlation of data from around the world. *European Journal of Environmental and Civil Engineering*, *23*(2), pp.193-211. doi.10.1080/19648189.2016.1275984.

[29] Selvam, J.D.R., Smart, D.S.R. and Dinaharan, I., 2013. Microstructure and some mechanical properties of fly ash particulate reinforced AA6061 aluminum alloy composites prepared by compocasting. *Materials & Design, 49*, pp.28-34. doi.10.1016/j.matdes.2013.01.053.

[30] Patil, S.R. and Motgi, B.S., 2013. A Study on Mechanical Properties of Fly Ash and Alumina Reinforced Aluminium Alloy (LM25) Composites. *IOSR Journal of Mechanical and Civil Engineering (IOSR-JMCE), 7(6),* pp.41-46.

[31] Bharat, N. and Bose, P.S.C., 2023. Corrosion Performance of AA7178 aluminum alloy reinforced with Sic nanoparticles. Materials Letters, *352.* p.135197. doi.10.1016/j.matlet.2023.135197

[32] Bharat, N. and Bose, P.S.C., 2022. Optimization of tribological behaviour of TiO2 nanoparticles reinforced AA7178 alloy matrix using ANN and Taguchi's methodology. *Surface Topography: Metrology and Properties, 10(2),* p.025032. doi.10.1088/2051-672X/ac7a55

[33] Bharat, N. and Bose, P.S.C., 2021. An overview on the effect of reinforcement and wear behaviour of metal matrix composites. *Materials Today: Proceedings. 46(1),* pp.707-713. doi.10.1016/j.matpr.2020.12.084.

[34] Michael Rajan, H.B., Ramabalan, S., Dinaharan, I. and Vijay, S.J., 2013. Synthesis and characterization of in situ formed titanium diboride particulate reinforced AA7075 aluminum alloy cast composites. *Materials & Design, 44*, pp.438-445. doi.10.1016/j.matdes.2012.08.008.

[35] Xavier, L.F. and Suresh, P., 2016. Wear Behavior of Aluminium Metal Matrix Composite Prepared from Industrial Waste. *Hindawi Publishing Corporation. The Scientific World Journal, 2016,* pp.1-8. doi.10.1155/2016/6538345.

[36] Karbalaei Akbari, M., Mirzaee, O. and Baharvandi, H.R., 2013. Fabrication and study on mechanical properties and fracture behavior of nanometric Al2O3 particle-reinforced A356 composites focusing on the parameters of vortex method. *Materials & Design (1980-2015)*, 46, pp.199-205. doi.10.1016/j.matdes.2012.10.008.

[37] Canakci, A. and Arslan, F., 2012. Abrasive wear behaviour of B_4C particle reinforced Al2024 MMCs. *The International Journal of Advanced Manufacturing Technology*, 63, pp. 785–795. doi.10.1007/s00170-012-3931-8.

[38] Singh, M., Prasad, B.K., Mondal, D.P. and Jha, A.K., 2001. Dry sliding wear behaviour of an aluminium alloy–granite particle composite. *Tribology International, 34(8),* pp.557-567. doi.10.1016/S0301-679X(01)00046-9.

[39] Ansary Yar, A., Montazerian, M., Abdizadeh, H. and Baharvandi, H.R., 2009. Microstructure and mechanical properties of aluminum alloy matrix composite reinforced with nano-particle MgO. *Journal of alloys and Compounds, 484(1-2)*, pp.400-404. doi.10.1016/j.jallcom.2009.04.117.

[40] Saravanan, S.D. and Kumar, M.S., 2013. Effect of mechanical properties on rice husk ash reinforced aluminum alloy (AlSi10Mg) matrix composites. *Procedia Engineering, 64*, pp.1505-1513. doi.10.1016/j.proeng.2013.09.232.

[41] Bharat, N. and Bose, P.S.C., 2023. Optimizing the Wear Behaviour of AA7178 Metal Matrix

Composites Reinforced with SiC and TiO_2 Nanoparticles: A Comparative Study Using Evolutionary and Statistical Methods. *Silicon 15(11),* pp.4703–4719. doi.10.1007/s12633-023-02395-6.

[42] Bharat, N. and Bose, P.S.C., 2023. Wear performance analysis and optimization of process parameters of novel AA7178/nTiO_2 using ANN-GRA method. *Proceedings of the Institution of Mechanical Engineers, Part E: Journal of Process Mechanical Engineering*, doi.10.1177/09544089231156074.

[43] Bharat, N. and Bose., P.S.C., 2023. Microstructure, texture, and mechanical properties analysis of novel AA7178/SiC nanocomposites. *Ceramics International, 49(12),* pp. 20637-20650. doi.10.1016/j.ceramint.2023.03.195.

[44] Sitdikov, V.D., Murashkin, M.Y., Khasanov, M.R., Kasatkin, I.A., Chizhov, P.S. and Bobruk, E.V., 2014, August. X-ray studies of aluminum alloy of the Al-Mg-Si system subjected to SPD processing. *In IOP Conference Series: Materials Science and Engineering (Vol. 63, No. 1, p. 012087). IOP Publishing.* doi.10.1088/1757-899X/63/1/012087.

[45] Rajmohan, T., Palanikumar, K. and Arumugam, S., 2014. Synthesis and characterization of sintered hybrid aluminium matrix composites reinforced with nanocopper oxide particles and microsilicon carbide particles. *Composites Part B: Engineering, 59*, pp.43-49. doi.10.1016/j.compositesb.2013.10.060.

[46] Kumar, J., Singh, D., Kalsi, N.S., Sharma, S., Pruncu, C.I., Pimenov, D.Y., Rao, K.V. and Kapłonek, W., 2020. Comparative study on the mechanical, tribological, morphological and structural properties of vortex casting processed, Al–SiC–Cr hybrid metal matrix composites for high strength wear-resistant applications: Fabrication and characterizations. *Journal of Materials Research and Technology, 9(6)*, pp. 13607-13615. doi.10.1016/j.jmrt.2020.10.001.

[47] Kumar, J., Singh, D., Kalsi, N.S., Sharma, S., Mia, M., Singh, J., Rahman, M.A., Khan, A.M. and Rao, K.V., 2021. Investigation on the mechanical, tribological, morphological and machinability behavior of stir-casted Al/SiC/Mo reinforced MMCs. *Journal of Materials Research and Technology, 12*, pp. 930-946. doi.10.1016/j.jmrt.2021.03.034.

[48] Singhal, C., Murtaza, Q., Alam, P. and Hasan, F., 2019. Structural and mechanical properties of microwave hybrid sintered aluminium silicon carbide composite. *Advances in Materials and Processing Technologies, 5(4)*, pp. 559-567 doi.10.1080/2374068X.2019.1636188.

[49] Chatterjee, A., Sen, S., Paul, S., Roy, P., Seikh, A.H., Alnaser, I.A., Das, K., Sutradhar, G. and Ghosh, M., 2023. Fabrication and Characterization of SiC-reinforced Aluminium Matrix Composite for Brake Pad Applications. *Metals, 13(3)*, p.584. doi.10.3390/met13030584.

[50] Ikubanni, P.P., Oki, M., Adeleke, A.A. and Omoniyi, P.O., 2021. Synthesis, physico-mechanical and microstructural characterization of Al6063/SiC/PKSA hybrid reinforced composites. *Scientific Reports*, *11(1),* 14845. doi.10.1038/s41598-021-94420-0.